

RADIOACTIVE IMPLANT INDUCED X-RAY EMISSION SPECTROMETRY

BY THE USE OF ^{67}Ga , $^{99\text{m}}\text{Tc}$, ^{111}In AND ^{201}Tl

Ryohei AMANO

*The School of Allied Medical Professions, Kanazawa
University, Kodatsuno 5-11-80, Kanazawa 920*

Induced X-ray emission spectrometry was examined by mixing a sample in solution with a radioisotope, which was used as a X-ray excitation source. The radioisotopes used were ^{67}Ga , $^{99\text{m}}\text{Tc}$, ^{111}In and ^{201}Tl . The copper, strontium, iodine, barium, lead and uranium solutions were used as the sample to be analyzed. The effective excitation efficiencies for each radioisotope were obtained.

The excitation geometry of the specimen to external source is a major parameter in determining the performance of "conventional" X-ray emission spectrometry. If the X-ray excitation source is inside the sample to be analyzed, the geometrical factor is maximized. Radioisotopes, which emit low energy radiations, are suitable to the in-situ X-ray excitation source. Low energy radiations emitted from the implant radioisotopes are effective to excitate the neighbor stable atoms. The atomic rearrangement processes involve their characteristic X-ray emissions. Hence both these X-rays, and the γ and X-rays from the radioisotope are emitted out of a sample to be detected simultaneously. Recently, Joyce *et al.* have studied the radioactive implant induced X-ray emission by using ^3H , ^{35}S and ^{125}I , and demonstrated that the implant source strength required is typically 10^3 less than what would be required with usual external sources.¹⁾

Generally, half-lives of the radioisotopes should be kept short to reduce the radiological hazard and problem of disposal. The radioisotopes used for *in vivo* nuclear medicine can be applicable to the radioactive implant source because they have the short half-lives and emit the relatively low energy photons. In this work, the radioactive implant induced X-ray emission spectrometry was examined by using ^{67}Ga (half-life, $T=78.3\text{h}$), $^{99\text{m}}\text{Tc}$ ($T=6.02\text{h}$), ^{111}In ($T=67.9\text{h}$) and ^{201}Tl ($T=73.0\text{h}$). The copper, strontium, iodine, barium, lead and uranium solutions were used as the sample to be analyzed.

The *in vivo* radiopharmaceuticals of ^{67}Ga , $^{99\text{m}}\text{Tc}$, ^{111}In and ^{201}Tl were used as the implant source by dilution with distilled water. The radioisotope solution of interest was added to three kind of weight of each sample. The radioactivity in the sample solution was kept between 18.5kBq ($0.5\mu\text{Ci}$) and 55.5kBq ($1.5\mu\text{Ci}$) to minimize spectrum distortion due to pulse pile up. The sample volume was held constant at $200\mu\text{l}$. In this counting conditions, the area of the induced characteristic X-ray peaks were

proportional to activity of the sample. The identification of characteristic X-rays by photon spectrometry was carried out with a pure Ge detector (16mm active diameter; 10mm active depth; 0.127mm Be window) coupled with a 4096-channel pulse-height analyzer. Detector resolution was 182eV FWHM at 5.9keV and 493eV FWHM at 122keV. All samples were counted for 10^3 s under the same geometrical conditions. The area of X-ray peaks were calculated using the computer programs.

The obtained radioactive implant induced X-ray emission spectra were shown in Figs. 1 and 2. The effective excitation efficiency, η_{eff} , was calculated by the following equation, $\eta_{\text{eff}} = N_c / (N_a \cdot N_d)$. N_c is the number of counts in X-ray peak, N_a is the number of atoms in the sample, and N_d is the total number of decays of radioisotope for the counting interval. The effective excitation efficiencies for each radioisotope were shown in Table 1.

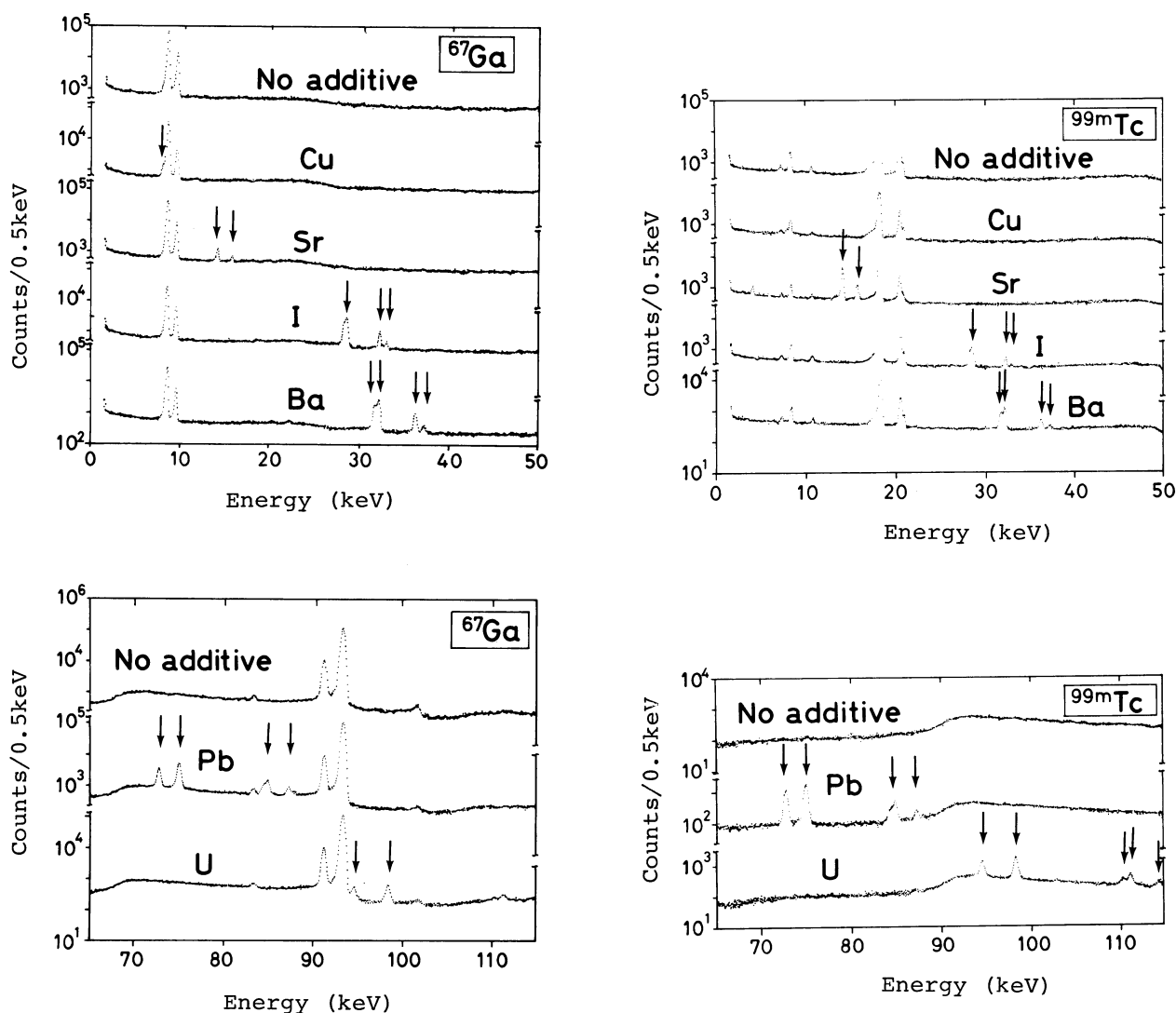


Fig. 1. The radioactive implant induced X-ray emission spectra by the ^{67}Ga and $^{99\text{m}}\text{Tc}$ sources. The weight of each additive is 10mg.

Arrows indicate the characteristic X-rays of the element of interest.

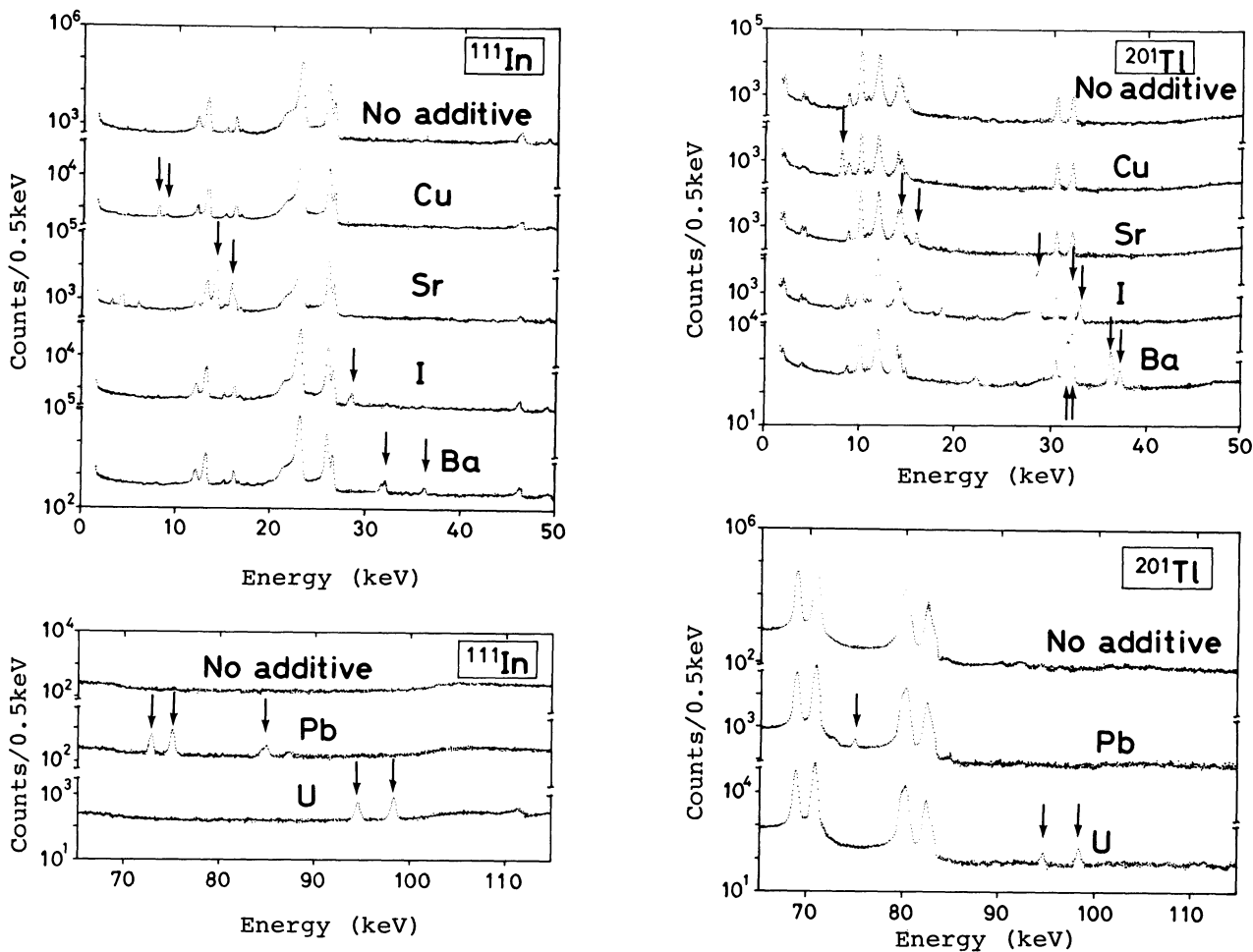


Fig. 2. The radioactive implant induced X-ray emission spectra by the ^{111}In and ^{201}Tl sources. The weight of each additive is 10 mg.

Arrows indicate the characteristic X-rays of the element of interest.

From these results shown in Figs. 1 and 2, and Table 1, the ^{67}Ga , $^{99\text{m}}\text{Tc}$, ^{111}In , and ^{201}Tl radioisotopes were found to be useful for the radioactive implant induced X-ray emission spectrometry. The elements which are most efficiently excited by each radioisotope are those whose K shell binding energy are just below the photon source energy. The $^{99\text{m}}\text{Tc}$ and ^{111}In sources were more efficient with elements above $Z=85$ than the other radioisotopes. In contrast with the cases of the $^{99\text{m}}\text{Tc}$ and ^{111}In sources, the ^{201}Tl source was more efficient with the elements between $Z=50$ and $Z=78$ than with lower and higher Z elements. On the other hand, the use of the pure Ge detector is not effective for the low elements below $Z=40$ because of its low counting efficiency for photon energy below 20 keV. A Si(Li) detector is preferable to the pure Ge detector for the application of the low Z coverage. Table 1 shows the relation of η_{eff} with weight of additive. The lack of constancy in η_{eff} with three kinds of additive weight is mainly caused by the difference of the self-absorption and scattering of the characteristic X-ray among the three samples. However, the self-absorption and scattering effect may be corrected by using the neighbor γ and X rays emitted from each radioisotope, whose relative intensities were determined previously.

Table 1. The effective excitation efficiencies, η_{eff} , for each radioisotope.

Sample	Characteristic X-rays Energy (keV)	$\eta_{eff} (10^{-25} \text{ Bq}^{-1})$			Sample	Characteristic X-rays Energy (keV)	$\eta_{eff} (10^{-25} \text{ Bq}^{-1})$		
		Sample mass					Sample mass		
		10mg	5mg	1mg			10mg	5mg	1mg
⁶⁷ Ga+Cu	8.0(K α 1+K α 2)	NC	NC	NC	^{99m} Tc+Cu	8.0(K α 1+K α 2)	NC	NC	NC
⁶⁷ Ga+Sr	14.2(K α 1+K α 2)	6.66	9.09	NC	^{99m} Tc+Sr	14.2(K α 1+K α 2)	4.94 $\times 10^1$	6.77 $\times 10^1$	9.96 $\times 10^1$
	15.8(K β 1)	2.15	NC	NC		15.8(K β 1)	1.13 $\times 10^1$	1.59 $\times 10^1$	NC
⁶⁷ Ga+ I	28.6(K α 1+K α 2)	5.21 $\times 10^1$	5.44 $\times 10^1$	6.70 $\times 10^1$	^{99m} Tc+ I	28.6(K α 1+K α 2)	2.93 $\times 10^1$	3.54 $\times 10^1$	NC
	32.3(K β 1)	1.03 $\times 10^1$	1.08 $\times 10^1$	NC		32.3(K β 1)	6.36	NC	NC
⁶⁷ Ga+Ba	31.8(K α 2)	6.62 $\times 10^1$	7.13 $\times 10^1$	NC	^{99m} Tc+Ba	31.8(K α 2)	3.88 $\times 10^1$	NC	NC
	32.2(K α 1)	6.45 $\times 10^1$	6.85 $\times 10^1$	6.83 $\times 10^1$		32.2(K α 1)	3.71 $\times 10^1$	4.28 $\times 10^1$	NC
	36.4(K β 1)	1.32 $\times 10^1$	1.40 $\times 10^1$	NC		36.4(K β 1)	7.98	NC	NC
⁶⁷ Ga+Pb	72.8(K α 2)	3.33 $\times 10^1$	1.51 $\times 10^2$	1.45 $\times 10^2$	^{99m} Tc+Pb	72.8(K α 2)	6.35 $\times 10^1$	6.69 $\times 10^1$	9.10 $\times 10^1$
	75.0(K α 1)	1.55 $\times 10^2$	2.55 $\times 10^2$	2.31 $\times 10^2$		75.0(K α 1)	1.03 $\times 10^2$	1.06 $\times 10^2$	1.34 $\times 10^2$
	84.4(K β 3)	4.56 $\times 10^1$	7.23 $\times 10^1$	NC		84.4(K β 3)	3.27 $\times 10^1$	3.77 $\times 10^1$	NC
	84.9(K β 1)	4.90 $\times 10^1$	7.95 $\times 10^1$	6.58 $\times 10^1$		84.9(K β 1)	3.27 $\times 10^1$	4.08 $\times 10^1$	NC
	87.3(K β 2')	1.66 $\times 10^1$	2.70 $\times 10^1$	NC		87.3(K β 2')	1.09 $\times 10^1$	NC	NC
⁶⁷ Ga+ U	94.6(K α 2)	9.84	NC	NC	^{99m} Tc+ U	94.6(K α 2)	7.40 $\times 10^1$	8.73 $\times 10^1$	NC
	98.4(K α 1)	2.16 $\times 10^1$	2.19 $\times 10^1$	NC		98.4(K α 1)	1.15 $\times 10^2$	1.29 $\times 10^2$	1.92 $\times 10^2$
	110.4(K β 3)	NC	NC	NC		110.4(K β 3)	2.92 $\times 10^1$	NC	NC
	111.3(K β 1)	9.22	NC	NC		111.3(K β 1)	3.23 $\times 10^1$	2.54 $\times 10^1$	NC
	114.5(K β 2')	NC	NC	NC		114.5(K β 2')	1.38 $\times 10^1$	NC	NC
¹¹¹ In+Cu	8.0(K α 1+K α 2)	1.39 $\times 10^1$	2.06 $\times 10^1$	NC	²⁰¹ Tl+Cu	8.0(K α 1+K α 2)	1.45 $\times 10^1$	2.55 $\times 10^1$	5.51 $\times 10^1$
¹¹¹ In+Sr	14.2(K α 1+K α 2)	3.29 $\times 10^2$	4.42 $\times 10^2$	5.82 $\times 10^2$	²⁰¹ Tl+Sr	14.2(K α 1+K α 2)	7.79 $\times 10^1$	1.62 $\times 10^2$	NC
	15.8(K β 1)	9.07 $\times 10^1$	1.40 $\times 10^2$	3.50 $\times 10^2$		15.8(K α 1+K α 2)	5.58	8.01	NC
¹¹¹ In+ I	28.6(K α 1+K α 2)	2.88 $\times 10^1$	3.21 $\times 10^1$	NC	²⁰¹ Tl+ I	28.6(K α 1+K α 2)	1.72 $\times 10^2$	2.12 $\times 10^2$	2.17 $\times 10^2$
	32.3(K β 1)	NC	NC	NC		32.3(K β 1)	3.38 $\times 10^1$	3.92 $\times 10^1$	4.86 $\times 10^1$
¹¹¹ In+Ba	31.8(K α 2)	3.25 $\times 10^1$	NC	NC		33.0(K β 2')	6.75	9.88	NC
	32.2(K α 1)	3.31 $\times 10^1$	NC	NC	²⁰¹ Tl+Ba	31.8(K α 2)	2.55 $\times 10^2$	NC	NC
	36.4(K β 1)	NC	NC	NC		32.2(K α 1)	2.32 $\times 10^2$	2.62 $\times 10^2$	3.02 $\times 10^2$
¹¹¹ In+Pb	72.8(K α 2)	5.25 $\times 10^1$	5.92 $\times 10^1$	NC		36.4(K β 1)	4.59 $\times 10^1$	5.00 $\times 10^1$	7.22 $\times 10^1$
	75.0(K α 1)	9.21 $\times 10^1$	9.68 $\times 10^1$	NC		37.3(K β 2')	4.57	1.08 $\times 10^1$	NC
	84.4(K β 3)	NC	NC	NC	²⁰¹ Tl+Pb	72.5(K α 2)	NC	NC	NC
	84.9(K β 1)	3.11 $\times 10^1$	3.61 $\times 10^1$	NC		75.0(K α 1)	1.06 $\times 10^1$	NC	NC
	87.3(K β 2')	NC	NC	NC		84.4(K β 3)	NC	NC	NC
¹¹¹ In+ U	94.6(K α 2)	7.22 $\times 10^1$	7.70 $\times 10^1$	NC		84.9(K β 1)	NC	NC	NC
	98.4(K α 1)	1.07 $\times 10^2$	1.36 $\times 10^2$	NC		87.3(K β 2')	NC	NC	NC
	110.4(K β 3)	3.01 $\times 10^1$	NC	NC	²⁰¹ Tl+ U	94.6(K α 2)	8.88	1.46 $\times 10^1$	NC
	111.3(K β 1)	2.39 $\times 10^1$	NC	NC		98.4(K β 1)	1.31 $\times 10^1$	1.33 $\times 10^1$	NC
	114.5(K β 2')	NC	NC	NC		110.4(K β 3)	NC	NC	NC
						111.3(K β 1)	NC	NC	NC
						114.5(K β 2')	NC	NC	NC

NC indicates that the efficiency was not calculated because the statistical error of the peak area is beyond 10%.

The present technique opens the possibility for *in vivo* nondestructive elemental analysis in the organ of interest.

Reference

- 1). J. R. Joyce, A. O. Sanni and E. A. Schweikert, *Nucl. Instrum. Methods*, **193**, 21(1982).

(Received June 19, 1982)